

# A Novel and Green Approach to Produce Nano-Porous Materials Zeolite A and MCM-41 from Coal Fly Ash and their Applications in Environmental Protection

K. S. Hui, K. N. Hui, and Seong Kon Lee

**Abstract**—Zeolite A and MCM-41 have extensive applications in basic science, petrochemical science, energy conservation/storage, medicine, chemical sensor, air purification, environmentally benign composite structure and waste remediation. However, the use of zeolite A and MCM-41 in these areas, especially environmental remediation, are restricted due to prohibitive production cost.

Efficient recycling of and resource recovery from coal fly ash has been a major topic of current international research interest, aimed at achieving sustainable development of human society from the viewpoints of energy, economy, and environmental strategy. This project reported an original, novel, green and fast methods to produce nano-porous zeolite A and MCM-41 materials from coal fly ash. For zeolite A, this novel production method allows a reduction by half of the total production time while maintaining a high degree of crystallinity of zeolite A which exists in a narrower particle size distribution. For MCM-41, this remarkably green approach, being an environmentally friendly process and reducing generation of toxic waste, can produce pure and long-range ordered MCM-41 materials from coal fly ash. This approach took 24 h at 25 °C to produce 9 g of MCM-41 materials from 30 g of the coal fly ash, which is the shortest time and lowest reaction temperature required to produce pure and ordered MCM-41 materials (having the largest internal surface area) compared to the values reported in the literature. Performance evaluation of the produced zeolite A and MCM-41 materials in wastewater treatment and air pollution control were reported. The residual fly ash was also converted to zeolite Na-P1 which showed good performance in removal of multi-metal ions in wastewater.

In wastewater treatment, compared to commercial-grade zeolite A, adsorbents produced from coal fly ash were effective in removing multi heavy metal ions in water and could be an alternative material for treatment of wastewater. In methane emission abatement, the zeolite A (produced from coal fly ash) achieved similar methane

removal efficiency compared to the zeolite A prepared from pure chemicals. This report provides the guidance for production of zeolite A and MCM-41 from coal fly ash by a cost-effective approach which opens potential applications of these materials in environmental industry. Finally, environmental and economic aspects of production of zeolite A and MCM-41 from coal fly ash were discussed.

**Keywords**—Metal ions; waste water; methane; volatile organic compounds.

## I. INTRODUCTION

ZEOLITE A and MCM-41 have uniform pore structure, large surface area and high thermal stability [1, 2]. For zeolite A, it has been manufactured industrially on a greater scale than any other zeolites [3]. The structure of zeolite A contains large cages having a near spherical shape of diameter of 11.4 Å. The effective pore size of zeolite A is 4 Å [1]. MCM-41 has a hexagonal structure with uni-dimensional pore structure with pore size ranging from 2-50 nm [2]. Several environmental and energy technologies can emerge with substantial benefits from zeolite A and MCM-41 materials, including basic science, petrochemical science, energy conservation/storage, medicine, chemical sensor, air purification, environmentally benign composite structure and waste remediation [4-8]. However, the use of zeolite A and MCM-41 in these areas, especially environmental remediation, are restricted due to prohibitive production cost [9].

Coal fly ash (CFA) is the waste product of combustion of coal in a coal-fired power station. The global annual production of CFA is about 800 million tons and this amount is predicted to increase in the future [10]. However, the global recycling rate of CFA is only 15% posing important challenges in waste management. At present, efficient disposal of CFA is a worldwide issue because of its massive production and its harmful effects on the environment [11]. Resource recovery from CFA can be one of the approaches to speed up reuse of CFA, since the major chemical compositions contained in CFA are SiO<sub>2</sub> and Al<sub>2</sub>O<sub>3</sub> (60-70 wt% and 16-20 wt%, respectively) [1]. Although CFA has

K. S. Hui is with Department of Manufacturing Engineering & Engineering Management, City University of Hong Kong, 83 Tat Chee Avenue, Kowloon Tong, Hong Kong.

K. N. Hui is with Department of Electrical and Computer Engineering, Rutgers, The State University of New Jersey, 94 Brett Road, Piscataway, New Jersey, 8854-8058.

Seong Kon Lee is with the Energy Policy Research Division, Korea Institute of Energy Research, 71-2, Jang-dong, Yuseong-gu, Daejeon, 305-343, Republic of Korea.

been reused in highway construction, land reclamation and restoration of eroded soil, the demand for such applications is still limited [12]. Converting CFA into useful zeolite A and MCM-41 materials is one of the approaches to recycle CFA. However, most of the studies applied a long conversion time (1-3 days) to produce zeolite and MCM-41 materials from coal fly ash and the materials produced still contained a significant amount of residual CFA [9, 13-15]. Thus, the potential applicability of the zeolite/MCM-41 materials is greatly reduced.

The presence of heavy metal ions in streams and lakes has been responsible for several types of health problems in animals, plants and human beings [16]. In wastewater treatment, zeolite A is a good adsorbent to remove metal ions in water because of its high cation exchange capacity. Methane is a potent greenhouse gas with a Global Warming Potential (GWP) 23 times greater than carbon dioxide [17]. In addition, methane is chosen as a model gas to represent volatile organic compounds (VOCs) which are a group of major air pollutants that have been associated with many health problems [1]. Zeolite A has been applied to adsorb methane [18]. In methane emission abatement by catalytic oxidation, zeolite A could be a good support to produce metal-ions exchanged catalysts because it has the highest cation exchange capacity and the largest number of acidity sites among other zeolites (zeolite X, Y, mordenite, ZSM-5, -11 and -48) [19]. However, there has been little investigation on using CFA converted zeolite A and MCM-41 (without residues of CFA) in wastewater treatment and in methane emission abatement. Removing heavy metal ions in contaminated water and abating methane emissions using low-cost materials may lead to substantial economic and environmental benefits. Knowledge on application of CFA converted zeolite/MCM-41-based materials in these topics could be useful in designing alternative cheaper wastewater treatment and air pollution control systems.

This report gives an overview of production of zeolite A and MCM-41 from CFA by a novel and green approach to reduce the energy consumed and the waste generated in the production process, which can be an important contribution to the large scale production of zeolite A and MCM-41 materials. Applications of the materials in wastewater treatment and air pollution control were reported. Environmental and economic aspects of conversion of CFA into zeolite A and MCM-41 were also discussed.

## II. EXPERIMENT

### A. Coal Fly Ash

The CFA used in this project was obtained from a power plant in the southern part of China and was used in each experiment after pretreatment at 120 °C for 30 min in an oven.

The size of the CFA, determined by a particle size analyzer (Coulter LS230), covers a range from 0.04 to 600  $\mu\text{m}$  and with an average diameter of 20.7  $\mu\text{m}$ . The chemical composition of the CFA was analyzed by XRF (JEOL JSX-3201Z) and is listed in Table I. The amounts of crystallized and amorphous  $\text{SiO}_2$  in the CFA are 3.9 and 46.2 wt% respectively, which was assayed by a quantitative X-ray diffraction (XRD) method [20]. The specific surface area of the CFA is 1.4  $\text{m}^2/\text{g}$ .

### B. Production of Zeolite A from Coal Fly Ash

A novel and fast method was developed to produce a pure form, single-phase and high-crystalline zeolite A from CFA compared to the methods reported in the literature [21]. Briefly, a mixture of 30 g of CFA and 300 ml of 2 M NaOH solution in a 1 l sealed polypropylene bottle was kept in an oil bath at 100 °C for 2 h under stirred conditions (300 rpm). Then, the solution was separated from the mixture by a filtration process. The molar ratio of  $\text{SiO}_2/\text{Al}_2\text{O}_3:\text{Na}_2\text{O}/\text{SiO}_2:\text{H}_2\text{O}/\text{Na}_2\text{O}$  in the solution was adjusted to 1.64:8.09:56.51 by adding 100 ml of aluminum solution. With the addition of the aluminum solution, single-phase and high-crystalline zeolite A could be easily produced from the solution compared to the case without the addition of the aluminum solution. The solution was then stirred (500 rpm) for 30 min at room temperature (25 °C) and kept at its first reaction temperature of 90 °C for 1.5 h and subsequently at the second reaction temperature of 95 °C for 2.5 h. The precipitated sample was separated from the mixture by a filtration process and washed with deionized water until the pH of the solution was around 10. The sample was kept in an oven and dried at 100 °C for 12 h. It took 6.5 h to produce 7.5 g of pure zeolite A powder from the CFA, denoted as CFAZA (coal fly ash zeolite A).

Compared with the zeolite A prepared under a constant reaction temperature, the proposed method (step-change of reaction temperature) reduced the total production time by half without compromising its quality. For example, as shown in Fig. 1, series 3 lead to higher crystalline zeolite A compared to series 4 and 5 if the reaction time in the second stage was in the range of 1–3 h. Series 3 also consumed less energy than series 5 in the production process. In addition, a narrower particle size distribution (PSD) of series 3 was obtained by applying the step-change of reaction temperature, as shown in Fig. 2. The step-change of reaction temperature during the production process may have the potential for producing a high crystalline and reduced particle size of zeolite crystal (series 3) which is a significant parameter that may affect the performance in several applications related to catalysis, diffusion, adsorption, ion exchange, etc. Detailed information

about the production of zeolite A from the CFA can be found in our previous work [21].

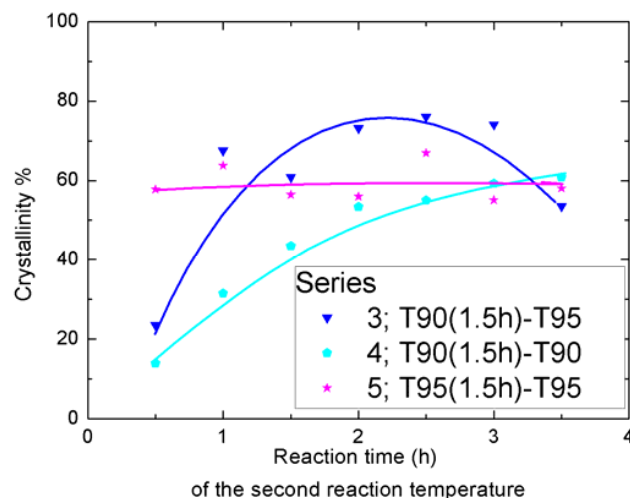


Fig. 1 The effect of step-change of reaction temperature on the percentage crystallinity of zeolite A

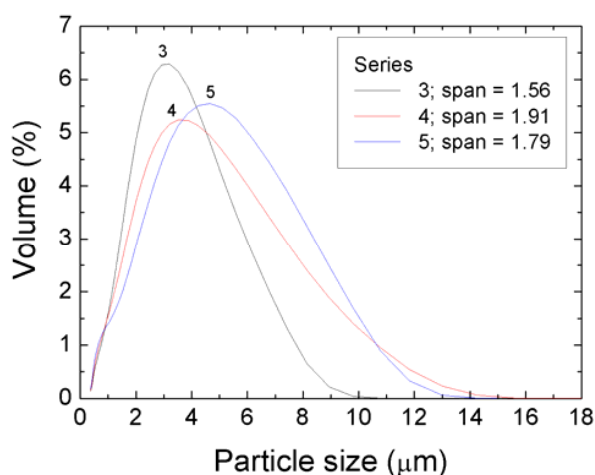


Fig. 2 Particle size distribution (PSD) curves of the zeolite A samples. Sample parameter: series 3 (T90(1.5h)-T95(3.5h)), series 4 (T90(1.5h)-T90(3.5h)) and series 5 (T95(1.5h)-T95(3.5h))

#### C. Production of MCM-41 from Coal Fly Ash

A green, cost-effective and fast method for production of MCM-41 was developed. Inexpensive coal fly ash as an inorganic silica source instead of expensive ones was used in the production process. Ethyl acetate ( $\text{CH}_3\text{COOC}_2\text{H}_5$ ) as a mild acid hydrolyser was used in the production of MCM-41 material under environmentally friendly conditions where no toxic waste was generated. This approach can be an important improvement to the industrial scale production of MCM-41 materials. The production process was carried out as follows [2]. The amorphous  $\text{SiO}_2$  component in the CFA was used as Si source for the production of MCM-41. **Extraction of Si**

**source:** Mixture of 30 g of CFA and 300 ml of 2M NaOH solution in a 1 l sealed PP bottle was kept in an oil bath at 100 °C for 4.5 h under stirred condition (300 rpm). Then the solution was separated from the mixture by a filtration process. The amounts of Si, Al and Na in the extracted solution (denoted as Si solution) were 5470 mg/l, 518 mg/l and 14900 mg/l, respectively (analyzed by ICP-AES, Perkin-Elmer 3000 XL). **Preparation of MCM-41 source solution:** MCM-41 source solution was prepared following the procedure described in the literature [22] with modification. At 85 °C and under stirring at 300 rpm, 82 ml of the Si solution was mixed with 1 g of CTAB to obtain an aqueous solution. Then, under stirring at 600 rpm, 3.1 ml of ethyl acetate was rapidly added into the solution. After stirring the mixture for 10 min, the obtained solution was cooled down to room temperature (25 °C) by natural convection. The resultant solution was denoted as M solution in this study. **Production of MCM-41:** 10 ml of M solution was adjusted to pH of 6.9 by the addition of a few drops of 5.25 N  $\text{H}_2\text{SO}_4$  solution under slow stirring (50 rpm). Precipitation was observed during pH adjustment. The pH adjusted solution was kept at room temperature (25 °C) for 24 h. The material obtained was washed with deionised water and dried at 100 °C for 2 h. The dried material was calcined under air at 550 °C for 4 h at a heating rate of 1 °C/min. The material was denoted as CFAMCM (coal fly ash MCM-41). Detailed information about the production of MCM-41 from the CFA can be found in our previous work [2].

#### D. Residual Coal Fly Ash

The residual CFAs from the production process of zeolite A and MCM-41 were also converted to another type of zeolite Na-P1 which showed good performance in removal of multi-metal ions in waste water [23].

#### E. Characterization of Samples

The pH values of the aqueous solutions were measured with a Mettler-Toledo meter (MP 120). The bulk elemental composition of the samples were determined by a JEOL X-ray reflective fluorescence spectrometer (XRF, JSX 3201Z). Powder X-ray diffraction (XRD) patterns of the samples were obtained using a powder diffractometer (Philips PW 1830) equipped with a  $\text{CuK}\alpha$  radiation. The accelerating voltage and current used were 40 kV and 20 mA, respectively. The scanning range of  $2\theta$  was set between 2° and 50°, with a step size of 0.02° and 0.01°/s. Nitrogen adsorption/desorption was carried out at 77 K using the Coulter SA3100 nitrogen physisorption apparatus. The volume of adsorbed nitrogen was normalized to standard temperature and pressure (STP). Prior to the experiments, the samples were dehydrated at 150 °C for 3 h. The BET surface area was determined from the linear part

of the BET plot ( $p/p_0 = 0.05-0.2$ ). Surface morphology of the samples was analyzed by scanning electronic microscopy (SEM, JEOL 6300) coupled with energy dispersive X-ray analysis (EDAX). In the SEM analysis, the samples were coated with a thin layer of gold and mounted on a copper stub using a double-stick tape.

The particle size measurements were performed by laser beam scattering technique (Coulter LS230). From the particle size distribution (PSD) curves obtained, the sizes of which 10%, 50% and 90% (by volume) of the particles in the samples were smaller could be determined. In this study, these particle sizes (by volume) were denoted by  $d(0.1)$ ,  $d(0.5)$  and  $d(0.9)$  respectively. The particle size of which 50% of the particles in the sample were smaller represented the average crystal diameter. Size span of the zeolite A samples were calculated by using the following equation:

$$\text{Span} = [d(0.9) - d(0.1)]/d(0.5) \quad (1)$$

where span is a measure of the width of the size distribution and smaller span values are obtained when narrower distribution exists.

All metal concentrations were analyzed using Inductively Coupled Plasma Atomic Emission Spectrometry (ICP-AES, Perkin-Elmer 3000 XL). The samples were usually diluted five times by deionized water. Therefore, the concentration of metal ion solutions should be in the range of 0–60 mg/l. The calibration standards were prepared using the standard solutions which was certified by the supplier. Three calibration standards (20, 40 and 60 mg/l) and blank solution were used to calibrate the equipment. A linear calibration curve was obtained after calibration. If the correlation coefficient  $R^2$  was less than 0.999, the machine was re-calibrated to ensure the accuracy of results. The samples were automatically measured three times in one aspiration. If the standard deviation of the test results were greater than 1%, the samples were measured again until the test results fulfilled the analysis requirement.

#### F. Waste Water Treatment

The experiments of sorption capacity were performed in a batch reactor (250 ml) at  $25 \pm 0.5$  °C with continuous stirring at 600 rpm. The adsorbents (0.01 or 0.5 g) were left in contact with 5 or 100 ml of multi-metal-ions solution in the range of each metal ions of 50 to 300 mg/l with the initial pH value of 3 for 240 min. The filtrates were filtered with 0.45  $\mu\text{m}$  filter and acidified with 2%  $\text{HNO}_3$  to decrease the pH to below 3 before the ICP-AES measurement. In order to obtain the sorption capacity, the amount of ions adsorbed per unit mass of adsorbent ( $q_e$  in milligram of metal ions per gram of adsorbent) was evaluated using the following expression:

$$q_e = \frac{C_0 - C_e}{m} V \quad (2)$$

where  $C_0$  is the initial metal ion concentration (mg/l),  $C_e$  is the equilibrium metal ion concentration (mg/l),  $V$  is the volume of the aqueous phase (l), and  $m$  is the amount of the adsorbent used (g). Removal efficiency of metal ions by the adsorbent is considered in percentage as:

$$\text{Removal efficiency} = \frac{C_0 - C_e}{C_0} \times 100 \quad (3)$$

#### G. Air Pollution Control

##### Preparation of multi-metal-ion-exchanged zeolite A.

Loading of the multi-metal-ions in the zeolite A (both commercial-grade zeolite A, Valfor 100, PQ Chemicals Thailand Limited and CFAZA) was achieved through an ion-exchange method [24]. The ion-exchange experiments, simultaneously performed in multi-ion solutions, were based on the information from our earlier study [23] that the selectivity sequence and the metal-loading capacity of the ions in zeolite A were dependent on the initial concentrations of the metal ions and the initial pH of the solution. Briefly, the selectivity sequence was  $\text{Cu}^{2+} > \text{Cr}^{3+} > \text{Zn}^{2+} > \text{Co}^{2+} > \text{Ni}^{2+}$  by zeolite A at the initial pH of 3. In the ion-exchange experiments, 0.5 g of the zeolite A was mixed with 100 ml of the multi-ion solution containing 5 mM of  $\text{Cr}^{3+}$ ,  $\text{Cu}^{2+}$ ,  $\text{Zn}^{2+}$ ,  $\text{Ni}^{2+}$  and  $\text{Co}^{2+}$  ions. These solutions were prepared by dissolving analytic-grade nitrate salts in deionized water. The initial pH of the mixture was adjusted to 3 by adding a few drops of 2%  $\text{HNO}_3$ . The mixture was mechanically stirred at 600 rpm at 25 °C for 24 h. No significant adsorption of the metal ions was found after 24 h of stirring. After the ion-exchange process, the final pH values of the solutions were 5.6. This is because the zeolite samples neutralized the solutions by acting as a proton acceptor [23, 25]. No precipitation of metal hydroxides was found. The ion-exchanged zeolite A powder was then filtered and washed by stirring in 1 l deionized water for 30 min. The zeolite A was then air dried at 110 °C for 12 h. The metal loaded zeolite A samples were labeled as Valfor 100-ML (Valfor 100-metal loaded) and CFAZA-ML (coal fly ash zeolite A-metal loaded), respectively.

**Experimental setup for air pollution control.** A schematic diagram of the experimental setup for this study is shown in Fig. 3. The methane conversion was evaluated in a 3.9 mm inner diameter and 600 mm long cylindrical quartz tube reactor heated by a temperature-controlled chamber, as used in our previous study [26]. Samples, in powder form (bed length of 1.5 cm), were loaded in the middle of the tube that was plugged with quartz wool at the two ends. The tube

was heated by infrared heaters placed above and under the tube. A K-type thermocouple was fixed to the middle of the sample bed to measure the reaction temperature and to control the reaction temperature to the set-point temperature. Before being loaded into the reactor, the sample was pretreated to ensure that its catalytic activity was representative, not due to the fact that it was 'fresh'. First, the sample was exposed to an air stream at a space velocity of  $41900 \text{ h}^{-1}$  at  $500^\circ\text{C}$  for 1 h (heated from room temperature to  $500^\circ\text{C}$  at a rate of  $10^\circ\text{C}/\text{min}$ ). The space velocity was defined as the total volume flow at the test temperature divided by the volume of the sample bed. Our previous works [24] have shown that  $500^\circ\text{C}$  was high enough to desorb any chemically adsorbed species in the sample. The sample was then aged at a space velocity of  $41900 \text{ h}^{-1}$  with 1 vol% methane for 6 h at  $500^\circ\text{C}$ . In all our tests, the relative humidity in the reactant stream was around 65%.

Methane conversion percentage was assessed on the basis of the percentage of carbon dioxide produced from the equation ( $\text{CH}_4 + 2\text{O}_2 \rightarrow \text{CO}_2 + 2\text{H}_2\text{O}$ ) under steady-state conditions. The reported values are the average of two sets of independent experiments using two different batches of pretreated sample. No methane conversion was detected in any of the tests using the empty reactor. No CO was detected in any of the tests.

### III. RESULTS AND DISCUSSIONS

#### A. Waste Water Treatment

Characterization of the adsorbents. Table I shows the chemical composition of the CFA, the treated CFA residue (TCFAR), the zeolite A produced from CFA (CFAZA), the Valfor 100 and the MCM-41 produced from CFA (CFAMCM). As shown in Table I, the BET surface area of TCFAR increased 13-fold from the CFA. This increase in BET surface area is due to crystallization of zeolite NaP1 crystals on the outer surface of the CFA. Although the CFAZA has a lower BET surface area than the Valfor 100, the BET surface area of CFAZA is similar to the value reported in literature [27]. The BET surface area of the CFAMCM is  $953 \text{ m}^2/\text{g}$ , which is higher than the reported value in literature [14].

Fig. 4 shows the morphology of the various adsorbents. The CFA consists of smooth spheres of diameter of  $0.04 - 600 \mu\text{m}$  and has a mean diameter of  $20.7 \mu\text{m}$ . These particles were formed from the cooling of molten products after the combustion of clay compounds in the original coal. By contrast, the morphology of the TCFAR was rough ( $1 - 10 \mu\text{m}$ , with a mean diameter of  $3 \mu\text{m}$ ), appearing as aggregates of small plates. This was because zeolite crystals (Na-P1) were precipitated out on the surface of the CFA particles. The morphology of the CFAZA and the Valfor 100 was chamfered-edged cube. The chamfered-edged cube

morphology was due to the initial  $\text{SiO}_2/\text{Al}_2\text{O}_3$  concentration used in the production process. The particle size of the CFAZA and the Valfor 100 were  $1-4 \mu\text{m}$  with a mean diameter of  $2.7 \mu\text{m}$  and  $1-3 \mu\text{m}$  with a mean diameter of  $2 \mu\text{m}$ , respectively. The particle size of the CFAMCM was around  $0.15 \mu\text{m}$ .

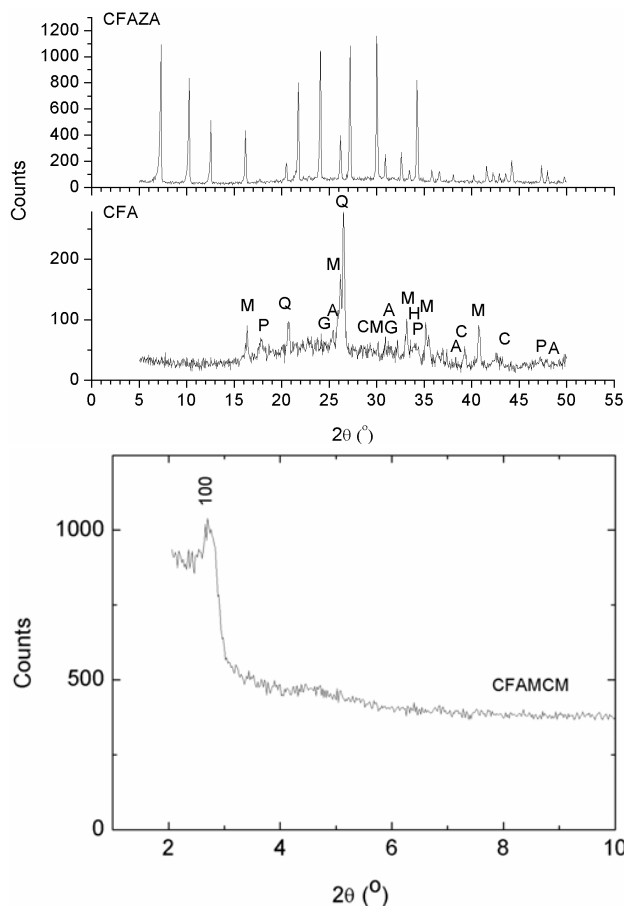


Fig. 5 XRD pattern of the CFA, CFAZA and CFAMCM. M, Q, C, P, A, H and G represent mullite, quartz, calcite, portlandite, anhydrite, hematite and gehlenite, respectively

Fig. 5 shows the XRD patterns of the CFA and the CFAZA, the crystalline species in the CFA sample are quartz, mullite, calcite, portlandite, anhydrite, hematite and gehlenite as identified by the sharp peaks, while the presence of the amorphous phases of  $\text{SiO}_2$  are identified by the presence of a broad diffraction peak (near  $2\theta = 24^\circ$ ). Quartz and mullite were produced during the thermal decomposition of clay minerals such as kaolinite during combustion. CFAZA was identified as a single phase zeolite A (JCPDS card 43-0142). The TCFAR was identified as a mixture of zeolite Na-P1 (JCPDS card 39-0219) and calcite ( $\text{CaCO}_3$ , JCPDS card 05-0586). Fig. 5 also shows the XRD pattern of the CFAMCM. The  $\{1\ 0\ 0\}$  reflection was observed, which represents the

characteristics of the hexagonal lattice symmetry of the MCM-41 structure.

**Sorption isotherm.** The analysis of the isotherm data is important to develop an equation which accurately represents the results and which could be used for design purposes. In order to investigate the sorption isotherm, two equilibrium models were analyzed: Langmuir and Freundlich isotherm equations. The Langmuir model is obtained under the ideal assumption of a totally homogeneous adsorption surface, whereas the Freundlich isotherm is suitable for a highly heterogeneous surface.

The Langmuir sorption isotherm is the best known of all isotherms describing sorption and it has been successfully applied to many sorption processes [28]. It is represented as:

$$q_e = q_m \frac{bC_e}{1 + bC_e} \quad (4)$$

where  $C_e$  is the equilibrium aqueous metal ions concentration (mg/l),  $q_e$  the amount of metal ions adsorbed per gram of adsorbent at equilibrium (mg/g),  $q_m$  and  $b$  the Langmuir constants related to the maximum adsorption capacity and energy of adsorption, respectively. The values of  $q_m$  (mg/g) and  $b$  (l/mg) can be determined from the linear plot of  $C_e/q_e$  versus  $C_e$ .

The Freundlich isotherm is most frequently used to describe the adsorption of inorganic and organic components in solution [29]. This fairly satisfactory empirical isotherm can be used for a non-ideal sorption that involves heterogeneous sorption and is expressed as:

$$\log q_e = \log K + \frac{1}{n} \log C_e \quad (5)$$

where  $K$  is roughly an indicator of the adsorption capacity and  $1/n$  the adsorption intensity. The magnitude of the exponent  $1/n$  gives an indication of the favorability of adsorption. Values of  $n$  where  $n > 1$  represent favorable adsorption condition. By plotting  $\log q_e$  versus  $\log C_e$ , values of  $K$  and  $n$  can be determined from the slope and intercept of the plot.

For all cases, the Langmuir model represents a better fit to the experimental data than the Freundlich model. The good agreement of the Langmuir plots with the experimental data suggests monolayer coverage of metal ions on the adsorbents. The values  $q_m$  and  $b$  obtained from these plots are listed in Table II. The Freundlich parameters  $K$  and  $1/n$  are also presented in Table II. The sorption sequence of the metal ions on zeolite A (CFAZA and Valfor 100) was the same and was as follows:  $\text{Cu}^{2+} > \text{Cr}^{3+} > \text{Zn}^{2+} > \text{Co}^{2+} > \text{Ni}^{2+}$ . More discussion about the observed sorption sequence can be referred to our previous study [23].

**Removal efficiency of multi-metal-ions by the CFA, TCFAR, CFAZA, Valfor 100 and CFAMCM.** The kinetics study showed that around 90% of the metal ions were removed in the first 60 min. No significant adsorption was detected after 240 min of stirring under all the experimental conditions. Table III lists the equilibrium sorption capacity of each metal ion by different adsorbents. The original CFA had the lowest equilibrium sorption capacity of the metal ions at the tested concentrations. Besides, it was interesting that the TCFAR had a relatively high equilibrium sorption capacity of the metal ions (except  $\text{Co}^{2+}$  ions) than zeolite A (CFAZA and Valfor 100). The high equilibrium sorption capacity of the metal ions by the TCFAR was caused by the high alkalinity of the sample (pH  $\sim$  11) and the existence of zeolite NaP1 on the outer surface of the sample. The main mechanisms of removal of metal ions by the TCFAR were due to adsorption and precipitation formation; while by the zeolite A (CFAZA and Valfor 100) were due to ion-exchange and adsorption.

Table III also shows that the CFAMCM (without any functional organic groups grafted onto the surface of the sample) are poor adsorbent for the removal of multi heavy metal ions. However, studies have shown that the sorption capacity of metal ions by MCM-41 samples can be significantly improved through post-modification of the MCM-41 samples to improve its affinity to metal ions. The CFAMCM possessed a large pore size, pore volume, BET surface area and good hydrothermal stability, as reported in our previous study [2]. These properties enabled them to accommodate a larger concentration of functional groups on their surface. It has been shown that the sorption capacity of metal ions increases with increasing concentration of the grafted functional group. It is expected that the CFAMCM can be used as an adsorbent in the treatment of waste water after grafting functional organic groups (such as thiol or amine) onto its surface. Based on the results, it was concluded that the TCFAR and the CFAZA could be applied for treatment of waste waters.

#### B. Air Pollution Control

**Characterization of the catalysts.** Table I shows the chemical composition of the metal-ions-loaded zeolite A catalysts (CFAZA-ML and Valfor 100-ML). Compared to their original forms, the slight decrease of elements such as Si and Al in the CFAZA-ML and Valfor 100-ML catalysts was due to partial dissolution of zeolite at the preparation conditions. The decrease of Na element in the CFAZA-ML and Valfor 100-ML catalysts was due to ion-exchange between the multi-metal-ions and the  $\text{Na}^+$  ions. The decrease in the BET surface area of the CFAZA-ML and Valfor 100-ML was due to the blockage of the pore structure of zeolite A by the exchanged metal ions.



**Methane emission abatement.** Experiments were conducted to compare the methane conversion efficiency of CFAZA-ML with that of Valfor 100-ML. A higher percentage methane conversion with the catalysts was achieved at lower space velocity, as shown in Fig. 6. This was due to the increased residence time for reactant molecules to diffuse to the active sites of the zeolite structure, and for diffusion of desorbed carbon dioxide and water from the active sites. This agrees with our previous study [26] showing that the diffusion limitation was predominant at 350-550 °C.

Experiments were then conducted to investigate the influence of methane concentration under different space velocities on methane conversion efficiency by the catalysts. The results are summarized in Table IV. The methane reaction rates with the catalysts (a mass of 0.18 g) were calculated based on the amount of carbon dioxide produced under the conditions tested. The methane reaction rates (in terms of mmol of methane converted/(g of sample x s)) increased with the inlet methane concentration under each space velocity. This was because the methane conversion rate depends on the concentration of the reactants. More methane reacted when the inlet methane concentration was higher. However, methane conversion decreased at higher inlet methane concentrations. This outcome was expected since the total number of active sites in the sample remained unchanged (the same amount of sample was used in the various experiments). Thus, when the amount of methane increased, there were not enough active sites available for the reactions at the same residence times [26].

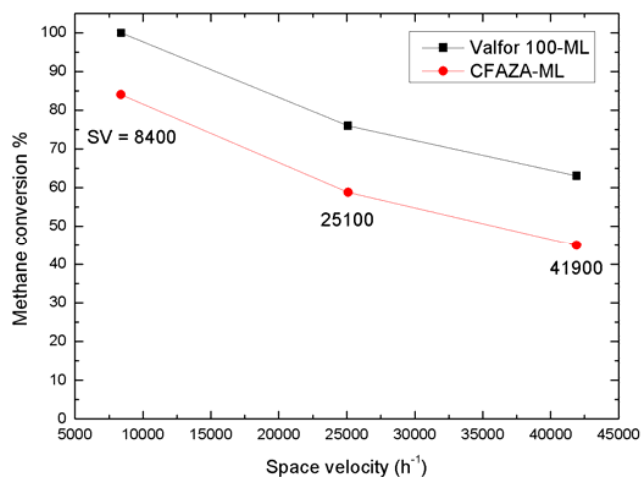


Fig. 6 The influence of space velocity on methane conversion percentage. Experimental conditions: inlet methane concentration of 1.1 vol%, reaction temperature of 500 °C and sample mass of 0.18 g.

The results in Table IV showed that the Valfor 100-ML achieved higher methane conversion percentages (2-24%)

than the CFAZA-ML under the conditions tested. These differences were attributed to the different percentages of metals loaded in the sample and the particle size of the sample. Taking into account the CFAZA-ML achieving a high methane conversion of 84% at low space velocity (such as 8400 h<sup>-1</sup>), applications of the CFAZA-ML in low-concentration methane emissions abatement under low space velocity seem to be promising.

Compared to other hydrocarbons, methane is considered the most difficult one to oxidize [30] and is often chosen as a model compound for evaluating the performance of catalysts tested in many volatile organic compound (VOC) abatement studies [31]. It seems that zeolite A catalysts prepared from CFA can be a low-cost VOC abatement option. The price of transition metals ions precursor per gram is cheaper than noble metals ions by 100-1000 times and that of CFA recycled zeolite A can be as low as 1 US\$/kg [32]. The cost of the multi-ion-exchanged zeolite A catalyst prepared from CFA can then be at least 70% lower than the commercial 2% Pd/Al<sub>2</sub>O<sub>3</sub> catalyst (11 US\$/g). The big cost difference indicates potential applications of CFA recycled zeolite in environmental industry.

#### C. Environmental and Economic Aspects of Production of Zeolite A and MCM-41 from Coal Fly Ash

Converting what was previously a waste material CFA from coal-burning power plants into zeolite A and MCM-41 may have several important implications on the environment and economy [32]. In terms of the environment, the increased use of CFA can reduce the need for additional landfill space and conserve natural resources. For example, a ton of CFA, compressed to 70 pounds per cubic foot, normally takes up approximately 28 cubic feet of landfill space. Each ton of recycled CFA reduces the use of one ton of virgin resources (e.g. limestone, gypsum, sand and soil) in the same applications [12]. It has been shown that CFA can be reused in highway construction, land reclamation and restoration of eroded soil [33]; however, the demand for reuse of ash in such projects is limited. Instead of dumping the ash in landfill sites or lagoons, converting it into zeolite and MCM-41 products can provide another way to protect the environment.

In term of the economy, zeolite produced from CFA can provide a new source of revenue for power production companies and eliminate previous expenses associated with the disposal of CFA. The residual ash, in which zeolite Na-P1 is formed on its outer surface is another value-added material. A detailed cost analysis of the feasibility of the production of zeolite A from coal fly ash can be referred to the literature [32]. Pure form zeolites produced from CFA may provide cost-effective alternative to commercial zeolites in

applications of pollution control and energy generation and storage.

#### IV. CONCLUSION

Many new developments in zeolite/MCM-41 science are driving the use of zeolites/MCM-41 as substitutes in many applications such as air and water purification, gases adsorption and catalysis. These developments include the development of new type of zeolite/MCM-41, production of zeolite/MCM-41 from waste materials and carbon-zeolite/MCM-41 hybrid materials. This project not only suggests novel and green methods to produce zeolite A and MCM-41 from CFA, but also provides two examples, in which zeolite A and MCM-41 were used for environmental protection. In views of environmental and economic aspects, production of zeolite A and MCM-41 from CFA may provide cost-effective alternative to commercial zeolites/MCM-41 in many applications.

#### ACKNOWLEDGMENT

Funding for this research was provided by the CityU SRG 7002470 and StUp 7200144.

#### REFERENCES

- [1] K.S. Hui, C.Y.H. Chao, "Methane emissions abatement by multi-ion-exchanged zeolite A prepared from both commercial-grade zeolite and coal fly ash," *Environmental Science & Technology*, 42, pp. 7392-7397, 2008.
- [2] K.S. Hui, C.Y.H. Chao, "Synthesis of MCM-41 from coal fly ash by a green approach: Influence of synthesis pH," *Journal of Hazardous Materials*, 137, pp. 1135-1148, 2006.
- [3] A. Dyer, *Introduction to Zeolite Molecular Sieves*, first ed., New York: Wiley, 1988.
- [4] C.T. Kresge, M.E. Leonowicz, W.J. Roth, J.C. Vartuli, J.S. Beck, "Ordered mesoporous molecular-sieves synthesized by a liquid-crystal template mechanism," *Nature*, 359, pp. 710-712, 1992.
- [5] X.S. Zhao, G.Q. Lu, G.J. Millar, "Advances in mesoporous molecular sieve MCM-41," *Industrial & Engineering Chemistry Research*, 35, pp. 2075-2090, 1996.
- [6] C.Y.H. Chao, C.W. Kwong, K.S. Hui, "Potential use of a combined ozone and zeolite system for gaseous toluene elimination," *Journal of Hazardous Materials*, 143, pp. 118-127, 2007.
- [7] C.W. Kwong, C.Y.H. Chao, K.S. Hui, M.P. Wan, "Removal of VOCs from indoor environment by ozonation over different porous materials," *Atmospheric Environment*, 42, pp. 2300-2311, 2008.
- [8] C.W. Kwong, C.Y.H. Chao, K.S. Hui, M.P. Wan, "Catalytic ozonation of toluene over zeolite and MCM type materials," *Environmental Science & Technology*, 42, pp. 8504-8509, 2008.
- [9] H. Misran, R. Singh, S. Begum, M.A. Yarmo, "Processing of mesoporous silica materials (MCM-41) from coal fly ash," *Journal of Materials Processing Technology*, 186, pp. 8-13, 2007.
- [10] L. Williams, "From coal dust to carbon credits," in *The University of New South Wales News*, 2008.
- [11] I. Twardowska, J. Szczepanska, "Solid waste: terminological and long-term environmental risk assessment problems exemplified in a power plant fly ash study," *The Science of the Total Environment*, 285, pp. 29-51, 2002.
- [12] E.P.A. US, "Using coal fly ash in highway construction: a guide to benefits and impacts," pp. EPA-530-K-05-002., 2005 [April].
- [13] X. Querol, N. Moreno, J.C. Umana, A. Alastuey, E. Hernandez, A. Lopez-Soler, F. Plana, "Synthesis of zeolites from coal fly ash: an overview," *International Journal of Coal Geology*, 50, pp. 413-423, 2002.
- [14] H.L. Chang, C.M. Chun, I.A. Aksay, W.H. Shih, "Conversion of fly ash into mesoporous aluminosilicate," *Industrial & Engineering Chemistry Research*, 38, pp. 973-977, 1999.
- [15] P. Kumar, N. Mal, Y. Oumi, K. Yamana, T. Sano, "Mesoporous materials prepared using coal fly ash as the silicon and aluminium source," *Journal of Materials Chemistry*, 11, pp. 3285-3290, 2001.
- [16] R.E. Clement, G.A. Eiceman, C.J. Koester, "Environmental-Analysis," *Analytical Chemistry*, 67, pp. R221-R255, 1995.
- [17] J.T. Houghton, Y. Ding, D.J. Griggs, M. Noguer, P.J. vandeLinden, D. Xiaosu, *Climate Change 2001: The Scientific Basis, Contribution of Working Group I to the Third Assessment Report of the Intergovernmental Panel on Climate Change*, Cambridge: Cambridge University Press, 2001.
- [18] J.A. Dean, *Lange's Handbook of Chemistry*, fifteenth ed., New York: McGraw-Hill, 1998.
- [19] E.M. Flanigen, "Zeolites and molecular sieves: an historical perspective," *Studies in Surface Science and Catalysis*, 137, pp. 11-35, 2001.
- [20] S.C. White, E.D. Case, "Characterization of fly-ash from coal-fired power-plants," *Journal of Materials Science*, 25, pp. 5215-5219, 1990.
- [21] K.S. Hui, C.Y.H. Chao, "Effects of step-change of synthesis temperature on synthesis of zeolite 4A from coal fly ash," *Microporous and Mesoporous Materials*, 88, pp. 145-151, 2006.
- [22] W.L. Dai, H. Chen, Y. Cao, H.X. Li, S.H. Xie, K.N. Fan, "Novel economic and green approach to the synthesis of highly active W-MCM41 catalyst in oxidative cleavage of cyclopentene," *Chemical Communications*, pp. 892-893, 2003.
- [23] K.S. Hui, C.Y.H. Chao, S.C. Kot, "Removal of mixed heavy metal ions in waste water by zeolite 4A and residual products from recycled coal fly ash," *Journal Of Hazardous Materials*, 127, pp. 89-101, 2005.
- [24] C.Y.H. Chao, K.S. Hui, W. Kong, P. Cheng, J.H. Wang, "Analytical and experimental study of premixed methane-air flame propagation in narrow channels," *International Journal of Heat and Mass Transfer*, 50, pp. 1302-1313, 2007.
- [25] A. Filippidis, N. Kantiranis, "Experimental neutralization of lake and stream waters from N. Greece using domestic HEU-type rich natural zeolitic material," *Desalination*, 213, pp. 47-55, 2007.
- [26] K.S. Hui, C.Y.H. Chao, C.W. Kwong, M.P. Wan, "Use of multi-transition metal-ion-exchanged zeolite 13X catalysts in methane emissions abatement," *Combustion and Flame*, 153, pp. 119-129, 2008.
- [27] H.L. Chang, W.H. Shih, "Synthesis of zeolites A and X from fly ashes and their ion-exchange behavior with cobalt ions," *Industrial & Engineering Chemistry Research*, 39, pp. 4185-4191, 2000.
- [28] N. Beyazit, O.N. Ergun, I. Peker, "Cu(II) removal from aqueous solution using Dogantepe (Amasya) zeolites," *International Journal of Environment and Pollution*, 19, pp. 150-159, 2003.
- [29] C. Namasivayam, R.T. Yamuna, J. Jayanthi, "Removal of methylene blue from wastewater by adsorption on cellulosic waste, orange peel," *Cellulose Chemistry and Technology*, 37, pp. 333-339, 2003.
- [30] J.H. Lee, D.L. Trimm, "Catalytic combustion of methane," *Fuel Processing Technology*, 42, pp. 339-359, 1995.
- [31] P. Hurtado, S. Ordonez, A. Vega, F.V. Diez, "Catalytic combustion of methane over commercial catalysts in presence of ammonia and hydrogen sulphide," *Chemosphere*, 55, pp. 681-689, 2004.
- [32] K.S. Hui, C.Y.H. Chao, "Pure, single phase, high crystalline, chamfered-edge zeolite 4A synthesized from coal fly ash for use as a builder in detergents," *Journal of Hazardous Materials*, 137, pp. 401-409, 2006.
- [33] T. Punshon, D.C. Adriano, J.T. Weber, "Restoration of drastically eroded land using coal fly ash and poultry biosolid," *The Science of the Total Environment*, 296, pp. 209-225, 2002.



TABLE I  
CHEMICAL COMPOSITION AND BET SURFACE AREA OF THE SAMPLES

Composition (wt%)	In Waste Water Treatment					In Air Pollution Control	
	CFA	TCFAR	CFAZA	Valfor 100	CFAMCM	CFAZA-ML	Valfor 100-ML
SiO <sub>2</sub>	50.09	43.34	43.34	44.68	95.17	35.17	36.31
Al <sub>2</sub> O <sub>3</sub>	24.91	35.71	35.71	34.91	1.16	30.49	29.89
Na <sub>2</sub> O	0.14	19.75	19.75	20.12	1.49	0.84	1.23
CaO	11.77	-	-	-	-	-	-
MgO	0.40	0.25	0.25	0.18	-	-	-
Fe <sub>2</sub> O <sub>3</sub>	7.60	0.80	0.8	-	-	0.74	-
Cr <sub>2</sub> O <sub>3</sub>	-	-	-	-	-	9.42	10.56
CuO	-	-	-	-	-	8.40	9.23
ZnO	-	-	-	-	-	4.72	3.87
NiO	-	-	-	-	-	1.82	0.93
CoO	-	-	-	-	-	2.01	1.22
BET surface area (m <sup>2</sup> /g)	1.4	22.2	54.8	71.4	953	37.0	38.0

- = not available

TABLE II  
LANGMUIR AND FREUNDLICH PARAMETERS FOR ADSORPTION OF MULTI-METAL-IONS ON ZEOLITE A

Adsorbent	Metal ions	Langmuir model			Freundlich model		
		q <sub>m</sub>	b	R <sup>2</sup>	K	1/n	R <sup>2</sup>
CFAZA	Co <sup>2+</sup>	13.7	0.3	0.998	6.7	0.2	0.959
	Cr <sup>3+</sup>	41.6	1.0	0.998	28.5	0.1	0.850
	Cu <sup>2+</sup>	50.5	2.2	1.000	37.1	0.1	0.974
	Ni <sup>2+</sup>	9.0	0.3	0.997	6.3	0.1	0.834
	Zn <sup>2+</sup>	30.8	0.2	0.995	18.5	0.1	0.623
Valfor 100	Co <sup>2+</sup>	11.5	1.2	0.997	4.8	0.2	0.911
	Cr <sup>3+</sup>	45.3	0.9	0.999	27.5	0.1	0.971
	Cu <sup>2+</sup>	53.5	0.5	0.997	36.9	0.1	0.965
	Ni <sup>2+</sup>	7.9	0.1	0.998	4.2	0.1	0.946
	Zn <sup>2+</sup>	31.6	0.3	0.997	17.6	0.1	0.871

Unit: q<sub>m</sub> (mg g<sup>-1</sup>), b (l mg<sup>-1</sup>), K (mg g<sup>-1</sup>)(mg l<sup>-1</sup>)<sup>n</sup>

R<sup>2</sup> is the correlation coefficient

Experimental conditions: T, 25 °C; stirring speed, 600 rpm; time, 240 min; pH, 3; V, 100 ml; m, 0.5 g of zeolite A

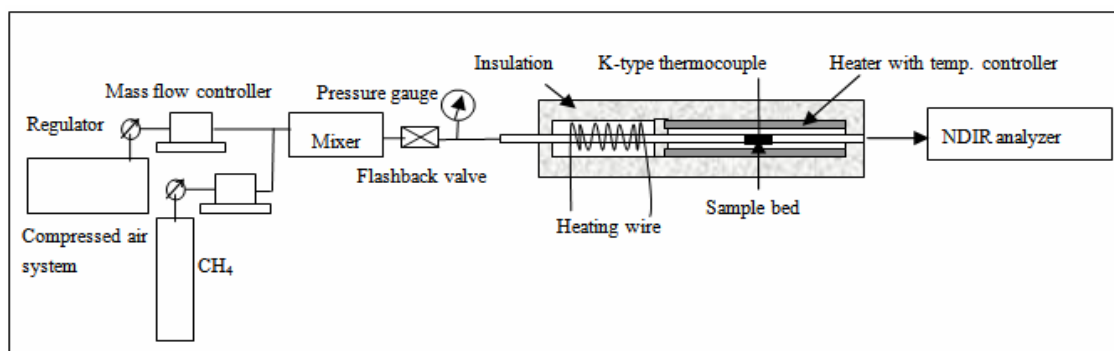


Fig. 3 A schematic diagram of the experimental setup

TABLE III  
EQUILIBRIUM SORPTION CAPACITY OF MULTI-METAL-IONS BY THE ADSORBENTS

Initial conc. (mg/l)	Adsorbent	Equilibrium sorption capacity <sup>a</sup>				
		Co <sup>2+</sup>	Cr <sup>3+</sup>	Cu <sup>2+</sup>	Ni <sup>2+</sup>	Zn <sup>2+</sup>
300	CFA <sup>b</sup>	1.2	10.0	15.2	2.0	4.0
	TCFAR <sup>b</sup>	8.8	48.7	55.0	9.2	30.3
	CFAZA <sup>b</sup>	13.5	41.6	49.9	8.8	27.0
	Valfor 100 <sup>b</sup>	11.2	44.5	51.1	7.6	25.8
	CFAMCM <sup>c</sup>	9.65	12.28	13.16	7.89	14.91

<sup>a</sup>Unit of equilibrium sorption capacity = mg/g

<sup>b</sup>Experimental conditions: T, 25 °C; stirring speed, 600 rpm; time, 240 min; pH, 3; V, 100 ml; m, 0.5 g.

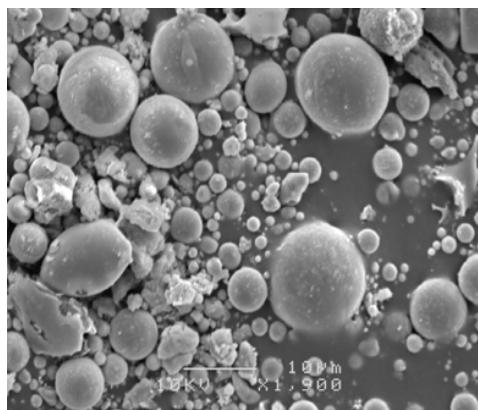
<sup>c</sup>Experimental conditions: T, 25 °C; stirring speed, 300 rpm; time, 240 min; pH, 3; V, 5 ml; m, 0.01 g

TABLE IV  
METHANE CONVERSION PERCENTAGE WITH THE SAMPLES AT 500°C

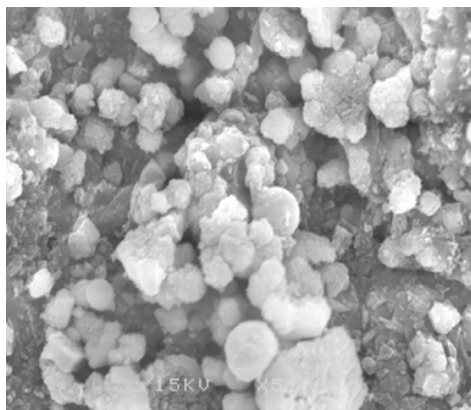
Space velocity/ Residence time (h <sup>-1</sup> )/(s)	Inlet CH <sub>4</sub> conc. (vol%)	Sample				
		Valfor 100-ML		CFAZA-ML		Control <sup>b</sup>
		Con%	Reaction rate <sup>a</sup>	Con%	Reaction rate	Reaction rate
8400/0.43	1.1	100	1.1E-03	84	9.1E-04	1.1E-03
	2.1	92	1.9E-03	68	1.4E-03	2.1E-03
	3.2	74	2.3E-03	58	1.8E-03	3.1E-03
25100/0.14	1.1	76	2.5E-03	59	1.9E-03	3.2E-03
	2.1	48	3.0E-03	49	3.0E-03	6.2E-03
	3.2	37	3.5E-03	34	3.2E-03	9.4E-03
41900/0.09	1.1	63	3.4E-03	45	2.4E-03	5.4E-03
	2.1	33	3.4E-03	22	2.3E-03	1.0E-02
	3.2	24	3.8E-03	22	3.5E-03	1.6E-02

<sup>a</sup> The unit of reaction rate is (mmol methane converted / (g of sample x s)).

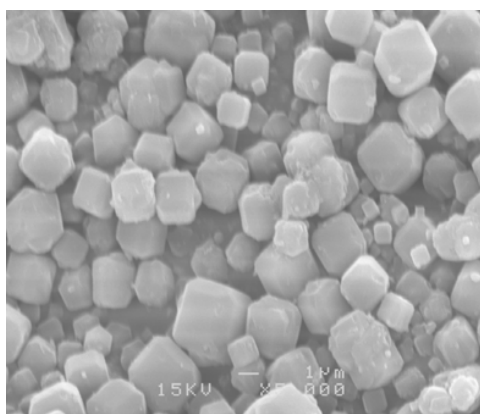
<sup>b</sup> Assumes a sample achieves 100 % methane conversion.



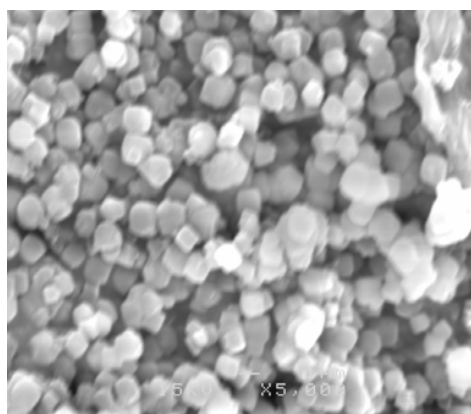
(a) CFA



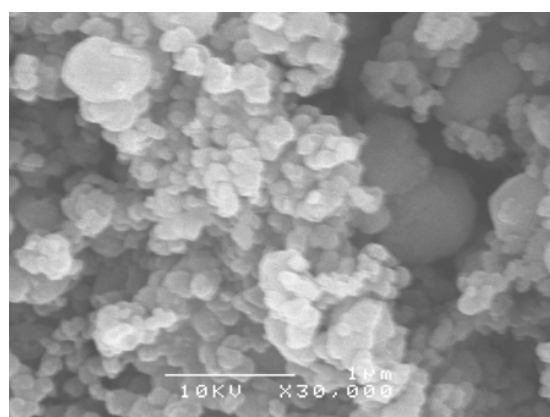
(b) TCFAR



(c) CFAZA



(d) Valfor 100



(e) CFAMCM

Fig. 4 SEM pictures of the adsorbents